

UDC 552.331:552.26+553.64(571)

## PETROCHEMICAL MODELS OF THE TOMTOR FIELD CARBONATITES (EASTERN SIBERIA)

**V. Vasilenko, L. Kuznetsova, A. Tolstov, V. Minin**

*V. S. Sobolev Institute of Geology and Mineralogy of SB RAS,  
3, Acad. Koptyug Av., 630090 Novosibirsk, Russia  
E-mail: vasilenko@igm.nsc.ru*

The chemical composition of the Tomtor field rocks has been investigated using the core of 193 boreholes located in the line crossing the rock mass from southeast to northwest. As many as 2 100 chemical analyses of rocks have been studied on the basis of system approach using the mathematical statistics methods to distinguish homogeneous rock groups composing the field. The database of chemical compositions was preliminarily divided into 43 groups by the cluster analysis method. The mean compositions of the groups within the  $\text{SiO}_2$ –( $\text{Na}_2\text{O}+\text{K}_2\text{O}$ ) diagram were concentrated within the boundaries of six discrete series. The first two series correspond to the compositions of alkali-syenite and alkali-gabbro, respectively, the third series – to melilite-like rocks, and the series from the fourth up to the sixth are presented by polygenetic carbonatites which we called polycarbonatites. All series could be characterized by extremely high variations of the compositions increasing from the third series towards the first and sixth series. The third series was considered as the parental one for the entire rock mass, it occurred as a result of selective melting of alkali-basalts under the conditions of  $\text{CO}_2$  saturation. The endogenous carbon dioxide was present at all rock formation stages.

The phosphorus behaviour has been specially studied. The petrochemical criteria for checking the genetic hypotheses of mineable phosphorus agglomerates formation were formulated. The presence of gravitational (residual) and metasomatic phosphorus agglomerates was defined in the rocks under investigation.

It is shown that the rock series have been distinguished reliably; similar petrochemical series take place in other apatite deposits, so they can also be used for geological mapping.

*Key words:* carbonatites, alkali rocks, ultrabasic rocks, system approach, mathematical statistics, genetic hypotheses, phosphorus deposits, Tomtor field, Eastern Siberia.

Based on the system approach and mathematical statistics, the authors of this study multiply used the results of routine X-ray spectrometry to analyze the contents of rock-forming oxides for system modelling of the rock bodies [11, 17, 18 et al]. The petrological verification of petrochemical models showed that using mass petrochemical information and mathematical statistics enabled to build demonstrative models of rock forming processes and substantial petrological interpretation of rocks. Thus, the

experience obtained makes it possible to rely on successful creation of petrochemical and petrological models of the Tomtor carbonatites.

**The Tomtor field.** The universal ores with respect to concentrations of the useful components and resources in epigenetically changed weathering cores of carbonatites were revealed in 1986 when carrying out the exploration operations within the central part of the Tomtor field (the Arctic zone of the Siberian platform). It is currently established that the basic resources of niobium and rare-earth elements associated with the Tomtor field are concentrated in the hypogene complex and epigenetic products of the weathering cores.

The Tomtor carbonatite and ultrabasic-alkali rock massif has an oval shape; it is over 20 km across and 250 km<sup>2</sup> in area. The petrographic and mineralogical data enable to distinguish central carbonatite core (40 km<sup>2</sup>) bordered by an incomplete ring of nepheline-pyroxene rocks (jacupirangites-ijolites) up to 3 km in width and the external ring up to 6 km in width, composed by alkali and nepheline syenites in the massif composition. According to the data of A. Tolstov, carbonatite breccias, ankerite carbonatites, ankerite-chamosite rocks, ore-bearing polymimetic carbonatites, apatite-microcline-micaceous rocks, ore-free polymimetic carbonatites, calcite-microcline-micaceous rocks, calcite-magnetite-ferruginous rocks (iron ores), ultrabasic rocks, alkali and nephelite syenites as well as foidolites can be distinguished in the massif composition.

The rock formation period is stretched in time from Vendian to Permian times; it is estimated as the Post-Devonian-Pre-Permian age [21]. Kaolinite-crandallite, siderite, gothite and francolite horizons (top to bottom) are distinguished in the hypogene complex. The epigenetically altered rocks of kaolinite-crandallite and siderite type are characterized by increased contents of niobium and rare-earth elements.

Geological, petrographic and mineralogical features of the rocks were described by a number of prominent researchers in numerous publications. The investigations of petrochemical composition of rocks carried out by earlier researchers are fragmentary and not used in our study.

**Original problem.** From the theoretical and practical perspectives, carbonatites are of interest for petrology and metallogeny. In the petrological respect, the petrochemical models should explain what the Tomtor massif carbonatites are and how they formed. The distribution of iron, manganese, phosphorus, niobium, rare-earth elements content in the varieties of carbonatites helps to solve metallogenic problems.

**Actual material.** The material used for this study was collected in the eighties of the past century, in the course of joint researches (on a cost accounting basis) of the Tomtor rock mass by the geologists of Chernyshevsk expedition (A. Orlov as the Customer's representative) and the Institute of Geology and Mineralogy, SB RAS, Novosibirsk (V. Vasilenko as the Contractor). To solve the original problem, 2 100 rock samples were taken from the core of 193 prospecting boreholes concentrated within one of the diameters dissecting the massif southwest to northeast. The contents of SiO<sub>2</sub>, TiO<sub>2</sub>, Al<sub>2</sub>O<sub>3</sub>, Fe<sub>2</sub>O<sub>3</sub>, FeO, MnO, MgO, CaO, Na<sub>2</sub>O, K<sub>2</sub>O, P<sub>2</sub>O<sub>5</sub> and LOI were defined in the samples. The content of CO<sub>2</sub> was additionally defined in 632 samples; the content of Nb<sub>2</sub>O<sub>5</sub> was defined in 566 samples. All researches were carried out in various certified laboratories of the former USSR.

**Methodological features.** Previously (Vasilenko et al., 1997), the methodology for building the system models based on the mathematical statistics was reviewed in detail. These models are difficult to apply due to the inconformity of empirical distributions of oxide concentration frequencies to the most widespread laws of random values distribution. These problems could be solved using the law of large numbers. When explaining this law, in the section “Statistic stability” Harold Cramer noted that “it is impossible to predict individual results in the succession of random experiments, since incorrect random combinations complicating the precise accounting are found in these results. However, as soon as we transfer our attention from the individual experiments to the succession of experiments in general, the situation will change radically and an extremely important phenomenon will occur: in spite of incorrect behaviour of individual results, the mean results of this sufficient succession of random experiments manifest striking stability” [7, p. 162]. The general population was divided by subpopulations using various algorithms. The statistic description of subpopulations was made traditionally, and the set of applied statistic tools remains unchanged in all our publications. Within the rock groups distinguished, the rock-forming oxides change their values from sample to sample in a different way; the ones with the generic character of change in concentration form a correlation complex. The correlation complexes can be distinguished using the method of correlation dendograms, which display the presence of complexes and their hierarchy. In this study, the correlation complexes were distinguished by the algorithms described in the work [12]. The correlation complexes of rock-forming oxides of magmatic rocks reflect jointly migrating parts of the medium from which they are formed.

**About the content of the term “carbonatite”.** The discussions on the issue “what is carbonatite” are well known, as well as the multiple arguments. The answer is unambiguous from the petrochemical viewpoint: if an oxide permanently occurs in the amounts more than 1 %, then it is rock-forming. This means, that all endogenous rocks containing more than 1 % of CO<sub>2</sub> on average are referred to carbonatites. However, in endogenous rocks carbonate can appear at all their formation stages, from the magmatic to the epigenetic one. In this connection, carbonatites should be considered as polygenetic formations [10, p. 365]. Later on, for all the varieties of the carbonatite association we shall use the term “polycarbonatites”, and the term “carbonatites” will define the formation type of polycarbonatite-containing complexes.

E. Epshtein and co-authors [9] were one of the first to use the CO<sub>2</sub> content to classify the carbonatites of the Tomtor massif. These authors subdivided the sampling of CO<sub>2</sub> contents in 658 analyses into silicate carbonatoids (CO<sub>2</sub> content from 0,2 to 14,0 %), carbonate-silicate carbonatoids (14–22), mesocratic carbonatites (22–34) and leucocratic carbonatites (34–43 %). Since the authors of this work did not have complete silicate analyses of the samples under study, the classification was not characterized appropriately from the petrochemical viewpoint.

For example, the compositions with the low CO<sub>2</sub> content are not necessarily the silicate ones.

Let us solve the problem of the Tomtor polycarbonatites classification based on the CO<sub>2</sub> contents repeatedly, using our material, by plotting the distribution of frequencies of CO<sub>2</sub> concentrations (Fig. 1).

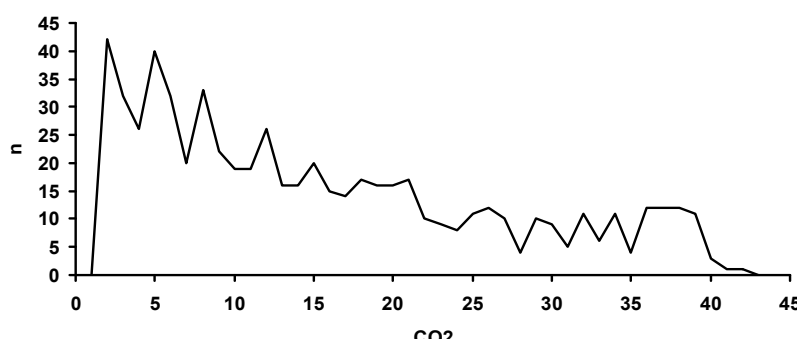


Fig. 1. Distribution of the values of CO<sub>2</sub> contents in the samples of Tomtor polycarbonatites:  
 n – number of samples.

The above succession has 11 modal compositions. If modal content reflects the composition of a certain variety of polycarbonatites, then, by comparing the compositions of all varieties (Table 1), it is easy to see that the succession in Fig. 1 includes three types of various polycarbonates. The subdivision into types is accentuated by mean contents of Fe<sub>2</sub>O<sub>3</sub>, FeO, K<sub>2</sub>O, and P<sub>2</sub>O<sub>5</sub>.

Table 1

Mean compositions of varieties (with respect to CO<sub>2</sub>)  
 of Tomtor field polycarbonates

Com- po- nents	Type I				Type II			Type III			
	I*	2	3	4	5	6	7	8	9	10	11
SiO <sub>2</sub>	16.42	10.93	13.56	10.08	9.14	6.42	6.23	5.44	5.14	3.73	2.93
TiO <sub>2</sub>	4.15	2.38	2.14	2.46	2.47	1.86	1.15	0.72	0.79	0.46	0.31
Al <sub>2</sub> O <sub>3</sub>	11.81	4.76	5.53	5.90	5.72	3.82	1.98	0.85	0.92	0.50	0.47
Fe <sub>2</sub> O <sub>3</sub>	18.48	24.10	18.64	19.28	16.32	11.61	5.85	3.31	3.55	2.49	1.72
FeO	5.63	7.61	11.26	11.67	18.13	23.75	23.26	9.24	4.64	4.21	3.70
MnO	0.95	2.39	3.22	4.86	3.21	3.61	2.96	2.81	2.13	1.63	1.52
MgO	1.70	1.46	1.92	1.85	1.76	1.97	2.85	6.25	4.20	3.71	3.72
CaO	9.49	15.86	12.99	10.56	9.49	10.10	16.99	31.31	37.92	41.44	43.17
Na <sub>2</sub> O	0.17	0.16	0.17	0.12	0.11	0.11	0.12	0.11	0.23	0.12	0.10
K <sub>2</sub> O	1.83	0.79	1.43	0.55	0.97	0.74	0.75	0.57	0.68	0.35	0.36
P <sub>2</sub> O <sub>5</sub>	11.35	12.00	9.34	8.71	6.36	4.95	3.23	2.91	2.83	3.46	2.70
CO <sub>2</sub>	1.23	4.16	7.97	10.49	13.35	18.89	25.04	28.70	31.38	33.47	36.40
<i>n</i> <sub>2 156</sub> **	86	115	86	29	71	102	40	20	21	14	48
Nb <sub>2</sub> O <sub>5</sub>	1.082	1.034	0.794	0.603	0.920	0.717	0.850	0.283	0.375	0.217	0.141
<i>n</i> <sub>565</sub> ***	85	92	74	31	57	89	32	13	15	9	26

\*I–II – varieties;

\*\**n*<sub>2 156</sub> – number of analyses from sampling of 2 156 analyses;

\*\*\**n*<sub>565</sub> – number of analyses from sampling of 565 analyses.

The antagonistic behaviour of calcium and magnesium carbonates in relation to other rock-forming oxides was the petrochemical trend defining the compositions of polycarbonates (Fig. 2). The number of varieties (see Table 1) occurred as a result of silicate rocks carbonatization.

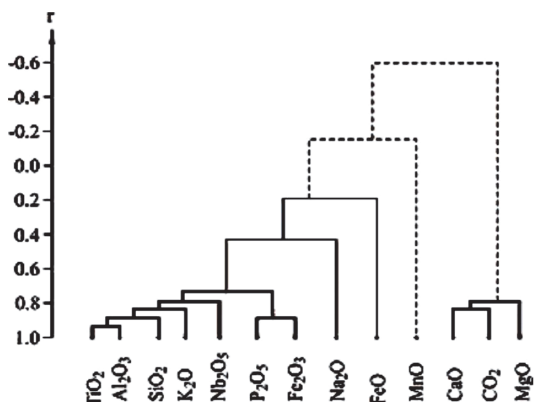


Fig. 2. Correlation dendrogram of mean compositions of varieties ( $n = 11$ ,  $r_{05} = 0.74$ ).

Here and below solid line means positive dependence, dotted line – negative.

In addition to Fig. 2, let us remark that the contents of  $\text{Nb}_2\text{O}_5$  are inversely proportional to the contents of  $\text{CO}_2$ . The regression equation has the following form:

$$f\text{Nb}_2\text{O}_5 = 1.09 - 0.024\text{CO}_2; r = -0.91.$$

Thus, all mineable chemical elements are correlated with the silicate part of rock.

However, this situation does not take into account post-magmatic processes, which could re-distribute the elements in polycarbonates. This could be studied taking into consideration all the analyses of general population of rock compositions of the Tomtor massif.

**Petrochemical model of the Tomtor massif.** Using the algorithm of dynamic cluster analysis [8], the population of chemical analyses of Tomtor rocks was subdivided into 43 cluster groups (Table 2) to build the model.

To analyze the interrelations of mean compositions of cluster groups, the diagram  $\text{SiO}_2-(\text{Na}_2\text{O}+\text{K}_2\text{O})$  was applied. This diagram was previously used by many researchers of magmatic rocks and made the basis of the work [6].

We also use this diagram by placing the imaging points of mean compositions of cluster groups on it (Fig. 3).

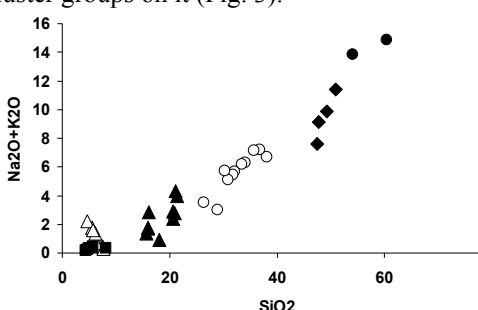


Fig. 3. Imaging points of mean compositions of cluster groups combined into six (1–6) series.

In Fig. 3 the imaging points of cluster mean values form an interrupted succession from substantially alkali and siliceous rocks to substantially carbonate ones. This succession has clear features of discreteness. In system analysis, the signs of discreteness are considered as the boundaries of separate populations (rock groups).

Table 2  
 Mean contents of oxides in cluster groups of Tomtor rocks

Com- po- nents	Series 1		Series 2				Series 3			
	1*	2	3	4	5	6	7	8	9	10
SiO <sub>2</sub>	60.46	54.08	50.87	47.83	49.32	47.15	38.14	36.82	35.69	34.08
TiO <sub>2</sub>	0.82	0.86	1.17	2.60	2.57	3.07	2.28	2.71	3.31	4.26
Al <sub>2</sub> O <sub>3</sub>	17.37	20.63	20.36	16.52	13.97	28.80	18.36	12.78	8.97	9.96
Fe <sub>2</sub> O <sub>3</sub>	1.79	2.44	2.69	5.42	5.67	1.33	2.85	3.45	3.10	17.60
FeO	1.40	2.65	3.46	3.87	4.84	0.79	5.89	4.83	6.80	5.38
MnO	0.29	1.17	0.18	0.41	0.31	0.06	0.37	0.34	0.41	0.72
MgO	0.88	0.40	1.02	1.48	2.64	0.27	3.74	5.65	8.27	4.15
CaO	0.60	0.96	2.36	2.49	4.05	0.39	5.38	12.95	8.07	6.65
Na <sub>2</sub> O	0.37	0.85	2.69	0.60	1.59	0.28	0.72	2.36	0.48	0.21
K <sub>2</sub> O	14.52	12.97	8.74	8.52	8.26	7.33	5.98	4.83	6.69	6.10
P <sub>2</sub> O <sub>5</sub>	0.26	0.29	0.28	1.44	0.53	0.79	2.34	2.50	1.56	4.40
LOI	1.27	3.70	5.19	8.86	6.29	9.70	13.86	10.79	16.60	6.55
Σ	100.10	100.00	100.10	100.00	100.01	99.99	99.36	100.01	99.95	100.05
n	4	34	15	51	15	47	30	29	24	21
CO <sub>2</sub>			0.20	0.45	0.51	4.77	4.14	4.22	1.66	
Nb <sub>2</sub> O <sub>5</sub>		Not analyzed		0.26	0.20	0.11	0.39	0.50	0.26	0.15
n'			6	1	16	2	2	5	26	

\* 1–43 – cluster groups.

Com- po- nents	Series 3								
	11	12	13	14	15	16	17	18	19
SiO <sub>2</sub>	33.47	32.12	31.86	30.83	30.26	29.23	28.23	28.98	26.34
TiO <sub>2</sub>	3.95	3.35	3.40	3.16	4.58	2.70	2.94	2.90	1.97
Al <sub>2</sub> O <sub>3</sub>	10.88	10.79	10.19	10.87	9.04	7.62	12.62	10.46	6.64
Fe <sub>2</sub> O <sub>3</sub>	13.88	5.92	8.29	10.89	3.35	2.99	6.82	19.25	39.36
FeO	7.24	5.95	6.80	6.81	17.09	6.48	18.43	11.93	5.79
MnO	0.83	0.50	0.84	0.86	1.08	0.55	0.95	0.40	0.57
MgO	5.07	8.44	8.56	6.07	6.03	7.83	4.85	7.57	0.70
CaO	6.12	11.93	10.32	9.53	4.60	15.18	3.96	5.09	2.38
Na <sub>2</sub> O	0.28	0.95	0.59	0.29	0.15	0.85	0.17	0.07	0.14
K <sub>2</sub> O	5.92	4.71	4.84	4.73	5.59	5.38	4.35	2.96	3.38
P <sub>2</sub> O <sub>5</sub>	4.49	2.68	3.49	5.46	3.22	2.69	3.49	2.95	1.76
LOI	7.88	12.57	10.77	10.35	14.96	18.34	13.01	7.91	10.96
Σ	100.00	99.57	99.95	99.85	99.94	99.84	99.94	100.49	99.96
n	64	136	126	39	48	95	23	6	2
CO <sub>2</sub>	4.01	5.89	3.58	2.48	7.43	11.13	3.51	Not analyzed	
Nb <sub>2</sub> O <sub>5</sub>	0.21	0.62	0.19	0.36	0.11	0.26	0.16	0.16	0.11
n'	20	10	10	5	8	6	11	1	1

On this basis, the succession in Fig. 3 can be subdivided into six series, i.e. rock groups of the Tomtor massif. It is possible to assume, that each series of successions of cluster mean values occurred as a result of separate phases of petrogenesis (Table 3).

The important signs of the distinguished series are the contents of rare elements in them.

The rest of Table 2

Com- po- nents	Series 4								
	20	21	22	23	24	25	26	27	28
SiO <sub>2</sub>	21.41	21.02	20.92	30.91	20.85	20.69	16.06	16.03	15.92
TiO <sub>2</sub>	2.40	2.11	1.78	5.96	4.18	2.30	1.40	2.68	1.67
Al <sub>2</sub> O <sub>3</sub>	6.01	6.01	4.75	15.23	11.19	5.96	3.86	7.02	3.64
Fe <sub>2</sub> O <sub>3</sub>	5.09	5.01	14.35	13.04	6.02	8.30	6.33	7.78	21.28
FeO	5.24	5.19	4.83	2.77	22.33	13.32	4.65	15.91	6.04
MnO	0.59	0.81	1.35	3.97	1.58	1.85	1.27	1.68	2.20
MgO	12.22	8.28	2.75	1.41	3.28	3.13	5.35	2.75	3.89
CaO	19.05	21.87	20.91	3.58	3.49	15.45	28.83	14.57	17.14
Na <sub>2</sub> O	0.51	0.32	0.21	0.14	0.12	0.22	0.26	0.20	0.20
K <sub>2</sub> O	3.46	3.97	2.59	1.07	2.26	2.69	2.56	1.51	1.57
P <sub>2</sub> O <sub>5</sub>	2.15	3.89	11.06	7.36	4.26	2.89	7.74	9.97	6.34
LOI	21.79	21.39	14.34	24.21	20.14	17.21	21.50	19.63	19.82
Σ	99.94	99.86	99.85	99.66	99.70	99.79	99.86	99.73	99.71
<i>n</i>	36	58	44	24	52	14	55	18	19
CO <sub>2</sub>	Not ana- lyzed	9.06	6.48	2.39	7.57	8.33	11.83	7.71	6.56
Nb <sub>2</sub> O <sub>5</sub>	0.42	0.51	1.31	0.54	0.26	0.35	0.53	0.57	
<i>n'</i>	11	19	11	11	10	25	9	9	9

Com- po- nents	Series 4					Series 5		
	29	30	31	32	33	34	35	36
SiO <sub>2</sub>	15.70	15.61	5.60	4.73	7.48	7.04	6.38	7.72
TiO <sub>2</sub>	4.27	6.44	0.70	0.40	6.55	1.71	1.25	1.39
Al <sub>2</sub> O <sub>3</sub>	12.18	15.99	1.30	1.01	19.83	1.92	2.07	1.72
Fe <sub>2</sub> O <sub>3</sub>	6.73	13.13	3.01	2.49	8.23	7.15	5.03	21.98
FeO	23.78	2.54	4.68	2.82	3.64	20.05	13.52	4.69
MnO	1.84	4.61	2.54	1.38	0.77	3.96	3.15	6.24
MgO	1.44	0.56	8.91	2.29	0.35	2.04	3.20	3.26
CaO	3.32	2.62	34.52	44.05	3.12	19.16	16.62	19.75
Na <sub>2</sub> O	0.20	0.17	0.12	0.16	0.20	0.17	0.12	0.16
K <sub>2</sub> O	1.16	0.46	1.64	2.08	0.25	0.35	0.56	0.15
P <sub>2</sub> O <sub>5</sub>	5.37	7.64	2.88	7.37	14.81	9.49	13.23	7.98
LOI	23.89	29.05	34.55	32.41	34.40	26.85	24.66	24.41
Σ	99.87	99.82	99.64	99.77	99.77	99.88	99.68	99.64
<i>n</i>	27	29	25	214	51	20	18	43
CO <sub>2</sub>	10.15	4.07	28.49	29.13	1.53	14.77	20.57	8.72
Nb <sub>2</sub> O <sub>5</sub>	0.64	1.68	0.26	0.37	2.34	0.76	0.46	0.83
<i>n'</i>	10	8	9	89	19	14	8	17

It follows from the Table 3 that the contents of Nb<sub>2</sub>O<sub>5</sub> in the groups from the second to the sixth of the series correlate with the mean contents of MnO, as well as high contents of Fe<sub>2</sub>O<sub>3</sub> and FeO in the sixth series, which is abnormally enriched in niobium. The correlation between the contents of CO<sub>2</sub> and Nb<sub>2</sub>O<sub>5</sub> is not statistically significant. In the rock mass from 39 contents of cluster groups (sampling from 565 analyses) and in the rock mass from five serial contents, the correlation coefficients make up 0.17 and 0.69, which is less than the allowable values for these numbers of observations ( $r_{01} = 0.41$  and 0.96, respectively).

End of Table 2

Components	Series 5		Series 6				
	37	38	39	40	41	42	43
SiO <sub>2</sub>	6.18	5.71	5.79	5.03	4.71	4.36	8.08
TiO <sub>2</sub>	0.94	0.58	2.54	2.37	1.80	1.64	3.86
Al <sub>2</sub> O <sub>3</sub>	1.60	1.07	5.94	6.00	3.20	2.24	4.36
Fe <sub>2</sub> O <sub>3</sub>	11.12	15.83	4.26	12.61	30.89	48.24	17.01
FeO	5.87	3.33	31.79	27.83	20.09	5.13	3.37
MnO	3.34	1.92	3.59	2.90	2.71	6.23	13.08
MgO	6.24	0.94	0.95	0.92	1.02	0.72	1.14
CaO	26.88	26.27	3.78	4.10	4.97	5.17	4.33
Na <sub>2</sub> O	0.15	0.21	0.13	0.12	0.12	0.12	0.16
K <sub>2</sub> O	1.19	1.38	0.30	0.23	0.10	0.07	0.19
P <sub>2</sub> O <sub>5</sub>	7.63	18.61	6.01	5.91	4.68	4.15	6.27
LOI	29.14	14.83	34.61	31.61	25.31	21.61	37.90
Σ	99.59	99.57	99.68	99.62	99.60	99.69	99.74
n	55	55	140	61	79	86	43
CO <sub>2</sub>	22.70	8.84	17.17	16.98	12.60	6.82	8.38
Nb <sub>2</sub> O <sub>5</sub>	0.56	0.83	1.07	1.21	1.17	1.17	2.09
n'	41	24	71	43	52	64	18

Table 3  
 Mean contents of oxides in series of cluster groups of Tomtor massif (2 154 analyses)

Components	Series					
	1	2	3	4	5	6
SiO <sub>2</sub>	54.75	48.11	32.47	18.98	5.77	5.41
TiO <sub>2</sub>	0.85	2.60	3.70	3.03	1.32	2.32
Al <sub>2</sub> O <sub>3</sub>	20.29	21.18	12.02	7.99	3.24	4.48
Fe <sub>2</sub> O <sub>3</sub>	2.37	3.63	6.45	8.78	7.67	21.21
FeO	2.52	2.81	7.68	9.28	4.68	23.30
MnO	0.19	0.24	0.63	1.75	2.27	4.87
MgO	0.45	1.12	6.44	4.69	2.83	0.93
CaO	0.93	1.89	8.70	15.15	32.51	4.41
Na <sub>2</sub> O	0.80	0.96	0.60	0.24	0.17	0.13
K <sub>2</sub> O	13.10	8.08	5.09	2.37	0.52	0.19
P <sub>2</sub> O <sub>5</sub>	0.29	0.96	3.13	6.47	9.60	5.37
LOI	3.39	8.41	13.00	21.11	29.12	29.94
n <sub>2</sub> 154	38	128	723	376	480	409
CO <sub>2</sub>	Not analyzed	1.73	5.03	8.24	18.30	14.55
Nb <sub>2</sub> O <sub>5</sub>		0.192	0.297	0.599	0.834	1.189
n <sub>565</sub>		23	107	92	160	184

The correlation between the compositions of the series and the types of polycarbonatites distinguished is characterized by the following features: (1) the share of polycarbonatites of the types I and II increases as the values of SiO<sub>2</sub> decrease; (2) polycarbonatites of the type III are present in the fifth series only.

Determination of how the polycarbonatites of various types form in succession is the important petrological problem. This can be determined by the example of compositions of rocks of the third series (Fig. 4).

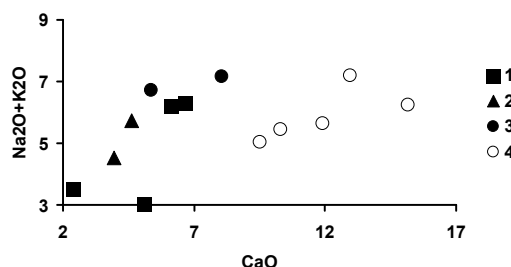


Fig. 4. Distribution of imaging points of mean compositions of cluster groups of the third series:

1–3 – group with low calcium content (1 – with high content of Fe<sub>2</sub>O<sub>3</sub> – cluster groups 10, 11, 18, 19 (see Table 2); 2 – with high content of FeO – cluster groups 15, 17; 3 – with Al<sub>2</sub>O<sub>3</sub> – cluster groups 7, 9); 4 – group with high calcium content – cluster groups 8, 12, 13, 14, 16.

Two successions of cluster groups can be distinguished here: *a* – with low calcium content, also including the compositions with Fe<sub>2</sub>O<sub>3</sub> and FeO prevailing and *b* – with high calcium content (see Fig. 4, Table 4).

Table 4

Mean compositions of four subgroups of the third series

Components	Series				Components	Series			
	1	2	3	4		1	2	3	4
SiO <sub>2</sub>	33.17	29.60	37.05	31.60	MgO	4.93	5.65	5.75	7.93
TiO <sub>2</sub>	3.91	4.05	2.74	3.16	CaO	6.09	4.39	6.58	12.00
Al <sub>2</sub> O <sub>3</sub>	10.55	10.20	14.19	10.05	Na <sub>2</sub> O	0.25	0.16	0.62	0.86
Fe <sub>2</sub> O <sub>3</sub>	15.61	4.48	2.96	6.26	K <sub>2</sub> O	5.72	5.19	6.29	4.91
FeO	7.09	17.53	6.30	6.32	P <sub>2</sub> O <sub>5</sub>	4.31	3.31	1.99	3.17
MnO	0.77	1.08	0.40	0.63	LOI	7.65	14.30	15.10	13.00
<i>n</i>	93	71	54	425	<i>n</i>	93	71	54	425

When studying polycarbonatites and associated alkali rocks, their mineralogical features are often used, among which feldspathoids play the main part. The most important mineralogical features of silicate rocks within the petrochemical study can be characterized by means of normative minerals. Using the algorithm for normative minerals calculation by Cross, Iddings, Pirsson and Washington (CIPW) [5], we recalculated 780 analyses of rocks of the first three series of the Tomtor field for normative minerals and averaged them within the cluster groups (Table 5). Leucite and nepheline were not found in the first series, in the second one they were found in separate cluster groups, and in the third series feldspathoids are present in all cluster groups.

By the relationship of alkalis and SiO<sub>2</sub> amount, cluster groups of the first series are identified as alkali-feldspathic syenite. The most characteristic distinctions of rocks of the first series from generic values [6] are variations of CaO and Al<sub>2</sub>O<sub>3</sub>. By the relationship of alkalis and SiO<sub>2</sub> amount, cluster groups of the second series relate predominantly to alkali gabbroids, such as essexites and shonkinites. The ordinary analyses reveal conformity with gabbro-anorthosites; at the same time, increased contents of Al<sub>2</sub>O<sub>3</sub> and decreased contents of CaO are characteristic for them. Based on petrochemical classification, the rocks of the second series should be related to alkali gabbroids with variations up to anorthosites.

Table 5  
 Mean contents of normative minerals in cluster groups of the first–third series

Minerals	Series 1		Series 2			Series 3.1				
	1*	2	3	4	5	6	19	18	11	10
Apatite	0.51	0.61	0.92	2.85	2.29	1.97	7.07	6.84	10.22	10.10
Ilmenite	0.77	1.61	1.49	7.41	2.12	5.55	3.73	5.51	7.42	7.22
Orthoclase	90.58	70.62	68.30	66.09	43.36	40.51	19.88	17.50	33.55	32.94
Leucite	0.00	0.00	6.39	0.05	0.02	0.01	0.00	0.00	1.26	2.05
Albite	0.00	1.25	0.98	1.21	4.75	2.54	1.19	7.65	1.59	0.95
Nepheline	0.00	0.01	1.34	0.01	0.01	0.02	0.00	0.00	0.41	0.47
Anorthite	0.74	2.57	3.72	0.42	6.57	-0.17	0.34	5.98	-0.83	-0.29
Magnetite	0.67	2.92	2.80	2.99	5.02	1.06	14.80	26.81	12.04	8.77
Hematite	0.38	0.36	0.77	2.19	2.39	1.91	29.16	0.78	5.61	11.54
Diopside	0.00	0.04	0.01	0.02	0.01	0.22	0.00	0.00	1.32	2.05
Hypersthene	2.44	1.01	1.01	3.27	4.42	2.40	1.74	20.50	6.00	4.42
Olivine	0.01	1.66	1.18	0.33	0.01	0.00	0.00	0.67	2.13	3.47
n	2	32	19	11	18	54	2	6	64	21

\*1–19 – cluster groups.

Minerals	Series 3.2		Series 3.3		Series 3.4				
	17	15	7	9	14	13	12	8	16
Apatite	7.31	7.51	3.58	3.45	11.45	8.50	5.89	5.80	6.71
Ilmenite	7.57	8.58	5.98	6.74	5.39	6.35	6.14	4.82	5.24
Orthoclase	18.73	15.90	24.73	11.30	21.77	17.27	10.92	9.13	2.21
Leucite	2.36	12.19	3.38	20.17	4.41	7.66	10.86	14.14	17.68
Albite	0.85	0.40	1.01	0.43	0.74	0.81	0.42	0.56	0.05
Nepheline	0.14	0.43	0.43	1.77	0.89	1.87	4.08	10.40	3.14
Anorthite	-3.19	0.00	1.34	1.70	1.89	4.40	5.21	7.33	2.21
Magnetite	11.39	4.70	2.30	4.09	10.92	9.12	6.71	4.10	3.70
Hematite	0.00	0.00	0.78	0.15	3.34	2.01	1.07	0.52	0.08
Diopside	0.05	1.44	1.01	5.45	2.82	4.74	6.03	16.50	4.69
Hypersthene	17.70	4.27	4.93	3.60	4.75	4.11	2.20	1.07	0.15
Olivine	13.35	24.17	7.95	10.36	8.63	12.08	12.37	3.83	16.73
n	23	48	30	24	39	126	136	29	95

The correlation analysis of rock-forming oxides and feldspathoids of the third series showed that calcium contents in the high-calcium subgroup correlated positively with the leucite contents; correlation with the elements of ferruginous group was not observed. High negative correlation with orthoclase was established in the subgroup with high calcium content.

Thus, calcium polycarbonatites occur first in the process of orthoclase removal and appearance of feldspathoids (Table 6).

The process of parallel formation of calcite polycarbonatites and feldspathoids took place during the active delivery of CO<sub>2</sub> into the system.

The general result of studying the correlation relationships between the contents of rock-forming oxides and normative minerals of the second and third series is shown on correlation profiles (Table 7) and correlation graph (Fig. 5).

The data obtained make it possible to conclude, that calcium carbonates and feldspathoids appear when CO<sub>2</sub> is delivered into the system, and orthoclase is removed from the system simultaneously.

Table 6

Coefficients of correlation of mean cluster contents of CaO and CO<sub>2</sub>  
 with mean cluster contents of normative minerals in the third series  
 $(n = 13, r_{01} = 0.68, r_{05} = 0.55)$

Components	CaO	CO <sub>2</sub>
Apatite	0.55	-0.23
Orthoclase	-0.75	-0.56
Leucite	0.66	0.27
Albite	-0.24	0.48
Nepheline	0.66	0.02
Anorthite	0.44	0.34
Magnetite	0.10	0.23
Hematite	-0.16	-0.35
Diopside	0.75	-0.07
Hypersthene	-0.11	0.24
Olivine	0.56	0.24
CaO	1.00	0.56
CO <sub>2</sub>	0.56	1.00

Table 7

Coefficients of correlation of mean cluster contents of CaO and CO<sub>2</sub>  
 with mean cluster contents of normative minerals in the second and third series  
 $(n = 17, r_{01} = 0.60)$

Components	CaO	CO <sub>2</sub>
Apatite	0.45	0.32
Orthoclase	-0.68	-0.72
Leucite	0.70	0.42
Albite	-0.06	0.17
Nepheline	0.70	0.17
Anorthite	0.49	0.26
Magnetite	-0.05	0.43
Hematite	-0.27	-0.17
Diopside	0.75	0.18
Hypersthene	-0.24	0.33
Olivine	0.50	0.51
CaO	1.00	0.61
CO <sub>2</sub>	0.61	1.00

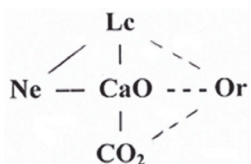


Fig. 5. Graph, demonstrating correlation relationships of mean contents of elements and normative minerals in rocks of the second and third series. Solid line means positive relationship, dotted line – negative.

Silicate rocks of the complex under study are exhausted by compositions of the third series. The fourth–sixth series are predominantly presented by carbonate types of polycarbonatites of metasomatic genesis, to a considerable degree.

The knowledge of composition of source rocks undergone carbonatization is important for the petrological model. The comparison of mean serial compositions of the Tomtor population under study with compositions of magmatic rocks of the known classification [6] showed that basalts and pyroxenites could be the source rocks for rocks of the third series. When comparing serial compositions with mean compositions of platform basalts [4, p. 133], it is evident (Fig. 6), that contents of CaO and Al<sub>2</sub>O<sub>3</sub> in rocks of the third series are within variations of mean compositions of these components for platform basalts.

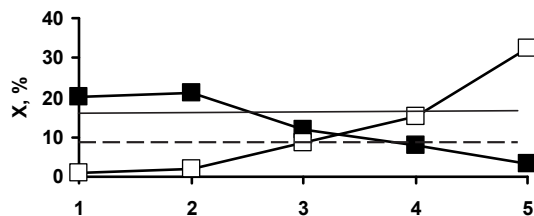


Fig. 6. Distribution of values of statistics of Al<sub>2</sub>O<sub>3</sub> and CaO oxides in series 1–5.

Squares designate imaging points of mean values: filled squares refer to Al<sub>2</sub>O<sub>3</sub>, transparent squares – to CaO; circles designate imaging points of mean coefficients of variation: filled circles refer to Al<sub>2</sub>O<sub>3</sub>, transparent circles – to CaO; solid line means statistic values of Al<sub>2</sub>O<sub>3</sub>, dotted line – statistic values of CaO for platform basalts [4].

The coefficients of oxides variation were the other argument in favour of the fact, that alkali basalts were the source rock for compositions of the third series. In the earlier publication of V. Vasilenko and co-authors [15], when studying stratified gabbro-norite pluton in Pansky Tundra, it was established that the main petrochemical trend of population under study was the antagonism of Al<sub>2</sub>O<sub>3</sub> (as well as Sr and Rb) on the one hand and MgO (as well as Cu, Co and Cr) on the other. With respect to variability character of contents of chemical elements, the section described is subdivided into several parts, where the area of 1 010–1 900 m is characterized by minimum values of variation coefficients and the area of 254–465 m – by maximum ones. In the first area, the compositions of rocks reflect the initial undifferentiated composition of the rock mass with minimum values of variation coefficients, and the area with maximum values of variation coefficients includes both undifferentiated and quite differentiated compositions containing copper-nickel mineralization.

In the example under consideration (see Fig. 6), the values of variation coefficients of rocks of the third series are characterized by maximum proximity to the values of variation coefficients of basalts. Nevertheless, the homogeneity of compositions of the third series is relative. The cluster groups of the series form an uninterrupted succession of compositions from melilites to melilitolites by the relations of alkalis and SiO<sub>2</sub> amounts. Only ninth cluster group corresponds to melilitolites on average, with respect to the contents of other oxides. However, ordinary analyses of these rocks correspond to neither melilitolites, nor to other ultrabasic rocks of alkali type (melilites, foidites and foidolites) with respect to the contents of Fe<sub>2</sub>O<sub>3</sub>, CaO and Al<sub>2</sub>O<sub>3</sub>. Mean compositions of other cluster groups neither correspond to petrochemical types of ultrabasic alkali composition. The rocks of the third series could be conventionally characterized as melilite-like formations with polycarbonatites. This is the result of

our current observations. The initial substrate, in which the processes of calcite polycarbonatites formation took place, corresponded to alkali basaltoids of potassic specification in all appearances.

Our representations on the massif genesis are conformable with the petrological model of carbonatite formation according to L. Perchuk. In 1982, he proposed the idea of fluid extraction of components from magma in the interaction with the magmas of transmagmatic fluids [16]; alkali-carbonate fluids can carbonatize both peridotite and basaltoid melts, alkalinizing the melts and extracting calcium remarkable by its great chemical affinity with carbon dioxide into the fluid. The relation between alkali-ultrabasic rocks and carbonatites can be explained by this particular process. In opinion of L. Perchuk, alkalinization of peridotite-basalts should be necessarily accompanied by phosphorization of peralkalic rocks.

The phosphorus distribution in polycarbonatite complexes is also important in studying the processes of their metasomatic and near-surface change. This is confirmed by the fact that not all carbonatite complexes are apatite-bearing. V. E. McKelvey [14] remarked, that 20 % of carbonatite rock masses were phosphorus-bearing. We were able to display, that the content of  $K_2O$  was the main factor in apatite distribution. Using Fig. 7, it is easy to predict the level of apatite potential of polycarbonatites.

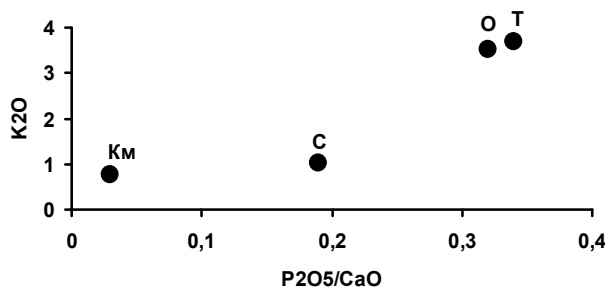


Fig. 7. Imaging points of mean compositions of complexes:

Km – kimberlites (ten pipes of diamondiferous kimberlites, 7 500 silicate analyses); C – Seligdar deposit (912); O – Oshurkovo deposit (193); T – Tomtor field (2 100 silicate analyses).

Prior to statement of the features of phosphorus distribution in the Tomtor massif, let us remind the basic hypotheses on the processes regulating the phosphorus distribution in polycarbonatites. We shall consider this problem in more detail using the ordinary analyses containing the estimates of  $CO_2$  in rocks of the fourth and fifth series. Before reviewing the actual material, let us remind the basic hypotheses on phosphorus distribution in polycarbonatites.

According to Z. Altschuller [1], two types of secondary phosphates are distinguished, i.e. residual and substituted phosphates. Residual phosphates are formed in precipitation of apatite as the heaviest mineral, in secondarily altered rocks. Iron-magnesium minerals, minerals of rare earths and niobium are accumulated in the process of gravitational differentiation jointly with phosphorus.

The representation on substance motion for specific geological objects at the time of their formation can be made on the basis of correlation of rock-forming oxides. Let

us consider the correlation relationships between rock-forming oxides for the typical cases of immersion and emersion in gravitational differentiation.

According to G. Baturin [3], the following phases are distinguished in present-day phosphate rock formation in oceanic shelf areas: phosphorus delivery to shelves by oceanic waters due to upwelling; consumption of phosphorus by organisms; precipitation of phosphorus to the bottom as a component of biogenic detritus, among which the organic substance plays the main part; diagenetic transition of phosphorus as a result of sulphate reduction from organic compounds to calcium phosphate, its dissolution in porous waters and precipitation when critical concentrations are reached. Gravity subsidence of apatite as the heaviest mineral of shelf sediments is the main thing in the mechanism of formation phosphorites generation. In dendrogram (Fig. 8) phosphorus-calcium complex (apatite) negatively correlates with the oxides of the remaining part of rock, in which alkali-carbon dioxide and aluminosilicate correlation kernels can be clearly distinguished. The presence of apatite antagonist is the main feature of correlation complexes of phosphate rocks, by which phosphate rocks can be identified.

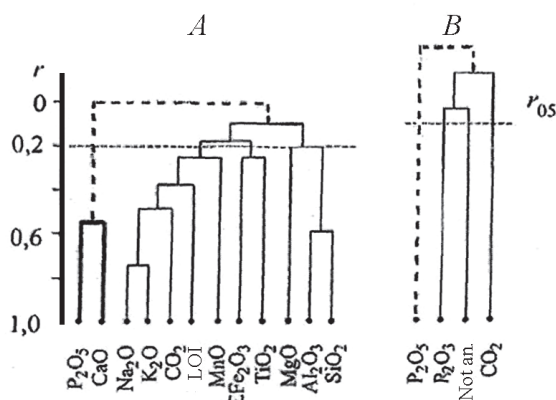


Fig. 8. Correlation dendograms of rock-forming oxides in phosphate rocks of shelves of present-day ocean (A) and phosphate series of the Chulaktau deposit (B). Coarse lines demonstrate phosphorus oxides antagonistic to other oxides [2].

Thus, apart from presence of other heavy minerals together with apatite, the sign of residual secondary polycarbonatites is also negative correlation of phosphorus with other oxides in statistical correlation analysis. In correlation dendograms this feature is reflected in the form of phosphoric correlation antagonist.

**Substituted or metasomatic phosphates.** The model of formation of rocks of this type was described by Z. Altschuller [1] by the example of deposits, which formed in the process of interrelation between ground waters enriched by phosphates and the products of limestone dissolution. Fluorapatites of endogenous origin are insoluble in hydrothermal-metasomatic process due to the high basicity of their solutions. Subsurface waters could become weakly acidic as a result of intensive dissolution of carbonates. Meteoric subsurface waters dissolve apatite and become enriched by  $P_2O_5$ . Weakly acidic solutions passing through phosphorus-enriched carbonate rocks be-

come weakly alkaline, being enriched by  $\text{Ca}^{2+}$ . The phosphorus solubility decreases again under these conditions, which results in apatite precipitation.

But this is other type of apatite. Fluorapatite gives place to carbonate fluorapatite or carbonate apatite, that's why there is no reason to speak about apatite reprecipitation. Thus, the metasomatic zones of increased phosphorus potential arise in the weathering cores of phosphate-bearing carbonate rocks (Table 8). For example, in Cooper rocks (Charleston, South Carolina) phosphatization is accompanied by intensive withdrawal of all components and input of phosphorus.

Table 8  
 Change in contents of  $\text{P}_2\text{O}_5$  and  $\text{CO}_2$  (wt. %) reflecting variations  
 of supergene phosphatization at depths of 7.05–9.30 m [1, p. 72]

Oxide	1	2	3	4	5	6	7	8	9
$\text{P}_2\text{O}_5$	9.6	5.2	3.8	3.2	2.8	2.4	2.1	2.4	2.1
$\text{CO}_2$	1.8	14.8	21.9	23.6	22.0	24.3	27.3	26.6	28.0

In the Tomtor field, the model of gravitational differentiation is shown most clearly in calcite polycarbonatites of the fourth series, which are characterized by 149 analyses, 36 of them include the data on the contents of  $\text{CO}_2$ :  $\text{SiO}_2$  – 19.29;  $\text{TiO}_2$  – 1.92;  $\text{Al}_2\text{O}_3$  – 5.22;  $\text{Fe}_2\text{O}_3$  – 5.51;  $\text{FeO}$  – 5.00;  $\text{MnO}$  – 0.93;  $\text{MgO}$  – 8.15;  $\text{CaO}$  – 23.76;  $\text{Na}_2\text{O}$  – 0.34;  $\text{K}_2\text{O}$  – 3.33;  $\text{P}_2\text{O}_5$  – 4.91; LOI – 27.47.

The correlation between the contents of  $\text{CO}_2$  and LOI is +0.82, which makes it possible to use the data on LOI along with the data on  $\text{CO}_2$ .

Sampling of Ca-polycarbonatites in the coordinates  $\text{P}_2\text{O}_5$ –LOI consists of two parts (Fig. 9, Table 9): with high and low contents of  $\text{P}_2\text{O}_5$ . We believe that high contents of  $\text{P}_2\text{O}_5$  arose as a result of gravitational differentiation under conditions of  $\text{CO}_2$  effect on polycarbonatites.

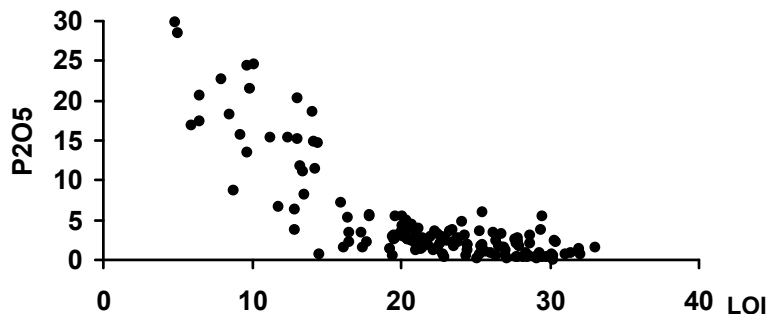


Fig. 9. Imaging points of compositions of Ca-polycarbonatites of the fourth series ( $n = 149$ ).

In his above work, Z. Altschuller made an assumption that such agglomerations of minerals heavier than calcite appear in dissolution of calcite. In the case under study, the correlation between the contents of  $\text{CaO}$  on one side and  $\text{CO}_2$  and LOI on the other is missing (Table 10), but strong negative relationships of  $\text{P}_2\text{O}_5$  with  $\text{CO}_2$  and LOI are present.

This gives the reason to conclude, that occurrence of high contents of  $\text{P}_2\text{O}_5$  took place in dissolution of calcite polycarbonatites as a result of influence of deep-seated emanations and precipitation of heavy minerals.

Table 9  
 Compositions of two groups of Ca-polycarbonatites of the fourth series

Components	Group	
	1	2
SiO <sub>2</sub>	17.68	19.78
TiO <sub>2</sub>	1.59	2.03
Al <sub>2</sub> O <sub>3</sub>	4.52	5.42
Fe <sub>2</sub> O <sub>3</sub>	9.50	4.67
FeO	4.82	5.06
MnO	1.62	0.77
MgO	5.19	8.91
CaO	25.85	22.95
Na <sub>2</sub> O	0.30	0.36
K <sub>2</sub> O	2.05	3.63
P <sub>2</sub> O <sub>5</sub>	16.14	2.21
LOI	10.63	24.11
<i>n</i>	27	122
Nb <sub>2</sub> O <sub>5</sub>	0.409	0.339
<i>n'</i>	13	12

Table 10  
 Correlation profiles of LOI and CO<sub>2</sub> in Ca-polycarbonatites of the fourth series

Components	LOI	CO <sub>2</sub>
SiO <sub>2</sub>	0.10	0.09
TiO <sub>2</sub>	0.17	0.38
Al <sub>2</sub> O <sub>3</sub>	0.05	0.21
Fe <sub>2</sub> O <sub>3</sub>	<b>-0.56</b>	-0.27
FeO	0.18	0.01
MnO	-0.20	-0.14
MgO	<b>0.27</b>	<b>0.48</b>
CaO	-0.25	-0.12
Na <sub>2</sub> O	0.02	-0.02
K <sub>2</sub> O	<b>0.37</b>	0.34
P <sub>2</sub> O <sub>5</sub>	<b>-0.78</b>	<b>-0.85</b>
<i>n</i>	149	36

As it follows from Table 9, Fe<sub>2</sub>O<sub>3</sub> and Nb<sub>2</sub>O<sub>5</sub> are also accumulated here, apart from phosphorus. These are so-called residual ores. Their origin due to gravitational differentiation is confirmed by the form of correlation dendrogram, where antagonistic behaviour of apatite-forming oxides (calcium and phosphorus) in relation to other oxides is clearly demonstrated, this is also shown by model example (Fig. 10).

Polycarbonatites of the first type contain less phosphorus than calcium polycarbonatites with a low content of volatile matters. In this case, the signs of gravitational differentiation are not clearly expressed: phosphorus and calcium associate with rock-forming oxides of silicate group; alkalis, oxides of iron, alumina and titanium associate with CO<sub>2</sub>; hence, they were removed from the system (Fig. 11).

Formation of high-phosphorous calcite polycarbonatites as a result of gravitational differentiation is evident. It is quite important to clarify the genesis of apatite agglomerations in low-phosphorous polycarbonatites. The collection of analyses of high-

calcium polycarbonatites of the fifth series with low content of phosphorus was made for this purpose. This collection includes predominantly the compositions of polycarbonatites of the third type.

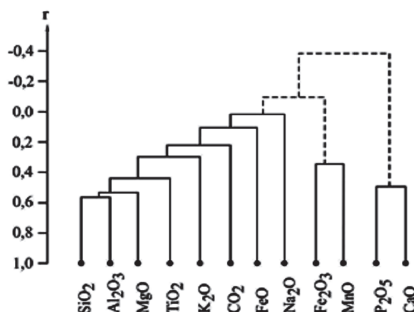


Fig. 10. Correlation dendrogram of rock-forming oxides of the third type of Ca-polycarbonatites of the fourth series in sampling containing  $\text{CO}_2$  ( $n = 36$ ,  $r_{01} = 0.44$ ).

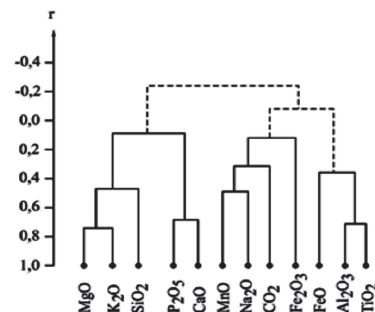


Fig. 11. Correlation dendrogram of rock-forming oxides of the first type of polycarbonatites of the fourth series.

The compositions of this collection contain up to 37 %  $\text{CaO}$  and 2.8 %  $\text{P}_2\text{O}_5$  on average ( $n = 131$ ):  $\text{SiO}_2 - 4.90$ ;  $\text{TiO}_2 - 0.69$ ;  $\text{Al}_2\text{O}_3 - 0.82$ ;  $\text{Fe}_2\text{O}_3 - 3.92$ ;  $\text{FeO} - 5.60$ ;  $\text{MnO} - 2.19$ ;  $\text{MgO} - 4.42$ ;  $\text{CaO} - 37.10$ ;  $\text{Na}_2\text{O} - 0.13$ ;  $\text{K}_2\text{O} - 0.52$ ;  $\text{P}_2\text{O}_5 - 2.81$ ;  $\text{CO}_2 - 30.50$ ;  $\text{Nb}_2\text{O}_5 - 0.685$ . The contents of  $\text{P}_2\text{O}_5$  could reach 9 %. As applied to this case, let us check the hypothesis on formation of apatite agglomerations, according to Z. Altschuller [1], by drawing up a correlation dendrogram of rock-forming oxides. Let us preliminarily remind that dissolution of apatite by acid solutions at the first stage and precipitation of apatite (of other type) with enrichment of the solution by calcite components is the key aspect in the hypothesis of metasomatic substitution of polycarbonate rocks. Thus, joint correlation of  $\text{CaO}$ ,  $\text{CO}_2$  and  $\text{P}_2\text{O}_5$  is a petrochemical sign of manifestation of metasomatic formation of apatite agglomerations. The correlation dendrogram of relationships between rock-forming oxides for the population of high-calcium and low-phosphorus polycarbonatites under study contains the evidence of their metasomatic genesis: the bond of  $\text{P}_2\text{O}_5$ ,  $\text{CaO}$  and  $\text{CO}_2$  is shown in dendrogram as the main antagonistic group, which makes it possible to accept a metasomatic hypothesis (Fig. 12).

Apart from the polycarbonatites of the third type, the polycarbonatites of the first type are widely spread in the fifth series. The study of correlation relations in sampling of these compositions showed, that formation of the polycarbonatites of the first type of this series took place analogously to what we described in the fourth series.

Alumino-ferruginous varieties of rocks occur in the fourth and fifth series jointly with polycarbonatites of various types. Substitution of aluminous rocks by the rocks enriched by ferrous iron and the low content of  $\text{CaO}$  are specific features of these rocks. In alumino-ferruginous-phosphate formations, the lack of lime is compensated by substitution of apatite and clay minerals by calcium and aluminum phosphates, such as crandallite, millisite and wavellite. In the correlation dendograms of rock-forming oxides this phenomenon is apparent, as phosphorus correlates with aluminum positively (Fig. 13). Alumino-phosphate rocks are formed with respect to the polycar-

bonatites of the first–third types, and in each case they retain petrochemical features of parent rocks.

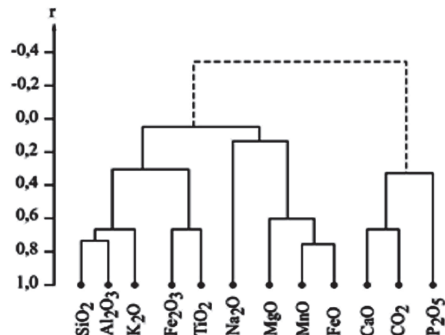


Fig. 12. Correlation dendrogram of rock-forming oxides in low-phosphorus polycarbonatites of the fifth series ( $n = 131$ ,  $r_{01} = 0.22$ ).

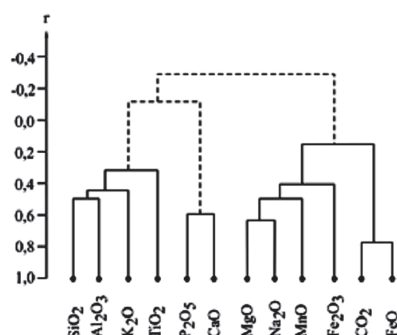


Fig. 13. Correlation dendrogram of rock-forming oxides in high-alumina rocks of the fifth series ( $n = 19$ ,  $r_{01} = 0.57$ ).

Polycarbonatites of the 6<sup>th</sup> series are represented by the first and second types of polycarbonatites (Table 11). Their correlation dendograms are remarkable by the fact, that they contain alumino-phosphate complexes of oxides, which can be considered as the evidence of their origination in the next (post-alumino-phosphate) phase (Fig. 14).

Table 11  
 Mean composition of polycarbonatites of the first and second types  
 of the sixth series in sampling containing CO<sub>2</sub>

Components	Types	
	I	II
SiO <sub>2</sub>	4.54	4.82
TiO <sub>2</sub>	1.85	2.52
Al <sub>2</sub> O <sub>3</sub>	2.77	5.97
Fe <sub>2</sub> O <sub>3</sub>	39.76	7.93
FeO	11.84	31.66
MnO	4.84	2.50
MgO	0.84	0.86
CaO	5.06	3.94
Na <sub>2</sub> O	0.10	0.11
K <sub>2</sub> O	0.07	0.21
P <sub>2</sub> O <sub>5</sub>	4.17	6.19
CO <sub>2</sub>	9.41	17.10
<i>n</i>	116	114

The presence of antagonistic correlation complex FeO–CO<sub>2</sub> with MnO adjoining is characteristic for polycarbonatites of the second type. Perhaps, this is the first evidence of transfer of MnO (and correlating content of Nb<sub>2</sub>O<sub>5</sub>) in carbonate metasomatism.

The bare presence of such correlation complex demonstrates the intensive development of sideriteization.

The correlation antagonist Fe<sub>2</sub>O<sub>3</sub> is present in polycarbonatites of the first type, which probably indicates intensive development of gothitization. Noteworthy is that

close negative dependence takes place between the contents of  $\text{FeO}$  and  $\text{Fe}_2\text{O}_3$ . The corresponding correlation coefficient equals  $-0.80$  at  $r_{01} = 0.16$ . Siderite polycarbonatites were substituted by the gothite ones, when physico-chemical conditions of rock formation changed.

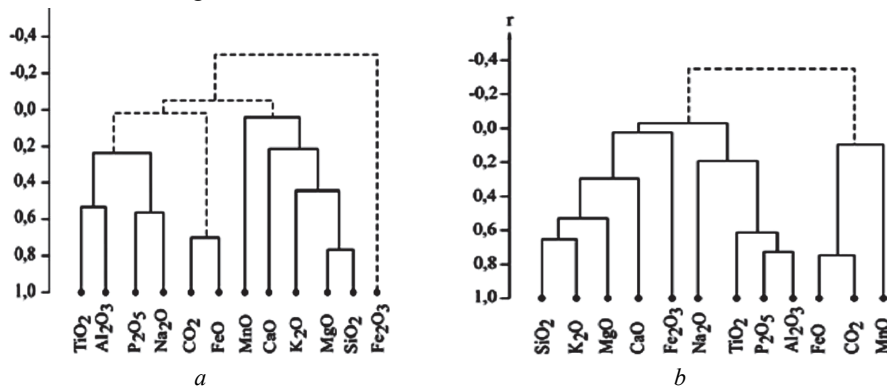


Fig. 14. Correlation dendograms of rock-forming oxides of the first (a;  $n = 114$ ) and second (b;  $n = 116$ ) type of polycarbonatites of the sixth series ( $r_{01} = 0.24$ ).

**Discussion.** According to Yu. Kuznetsov [13], the Tomtor massif with substantially potassic rocks relates to the formation of central intrusions of alkali and ultrabasic rocks with carbonatites.

The system analysis of the database of chemical compositions in the amount of 2 100 analyses of the complex rocks showed, that the complex includes six discretely separated series of compositions combining unified evolutionary succession from silicate high-alkali to carbonate low-alkali compositions.

This succession is not similar to petrochemical evolutionary trends according to, for example, by A. Zavaritsky [22], excluding kimberlites.

According to our data (Vasilenko et al., 1997), the compositions of magmatic complexes of kimberlites evolved from the carbonate to silicate varieties.

Based on the above information, it is possible to conclude, that evolution of compositions of the rocks of Tomtor massif from the rocks of the third series and proceeded towards polycarbonatites from the fourth up to the sixth series.

An exclusively high variability unparalleled in magmatic complexes is characteristic for serial compositions of rocks of the complex.

High variability of rocks of the third series increases by the beginning and by the end of evolutionary curve.

The fact of existence of magmatic complexes of ultrabasic-alkali rocks noted by many researches calls in question. We observed the presence of various rocks of carbonate, ferruginous and alumina compositions instead of them.

It appears that the third series was the source of various polycarbonatites of the Tomtor massif, which appeared due to selective melting of alkali basalts and other rocks of oceanic crust displaced to the upper parts of the Earth's crust by subduction processes. Melting took place under conditions of high saturation of magma-forming substrate by carbon dioxide, which was delivered by the mantle plume with other fluids.

The presence of relationship between phosphorus and potassium observed at the formation level was the result of extraction abilities of the alkaline medium.

High activity of  $\text{CO}_2$  at all stages of polycarbonatites formation should also be noted: in association with  $\text{CaO}$  at early high-temperature stages and in association with  $\text{FeO}$  at late high-temperature stages.

It stands to reason, that formation of the weathering core on polycarbonatites took place also with participation of  $\text{CO}_2$ , which arrived from deep-seated mantle sources.

The conclusion about participation of deep-seated sources of substance in formation of the nontronite profile of the weathering cores of the Southern Urals serpentinites was made by V. Razumova [19] within the context of hydrothermal-vadose hypothesis.

V. Vasilenko and co-authors [20] came to the conclusion that high contents of alumina in the weathering cores of kimberlites could not arise in eluvial enrichment, they were brought by hydrothermal solutions.

The participation of  $\text{CO}_2$  from the mantle sources at all stages of the Tomtor complex formation underlines the unity of its origination and formation processes.

The statistical method for distinguishing the series of chemical compositions of rocks of the Tomtor field requires a reliable verification.

Such verification was performed by taking 200 samples of core from 22 previously tested and four new boreholes, analyzing these samples chemically and subsequent inserting of the imaging points of ordinary analyses on the diagram  $\text{SiO}_2$ – $(\text{Na}_2\text{O}+\text{K}_2\text{O})$ .

Figure 15 depicts, that distribution of the points of ordinary analyses reproduces the serial structure of compositions from the collection numbering 2 100 analyses almost completely.

Distinguishing of the series of compositions can be considered reliable.

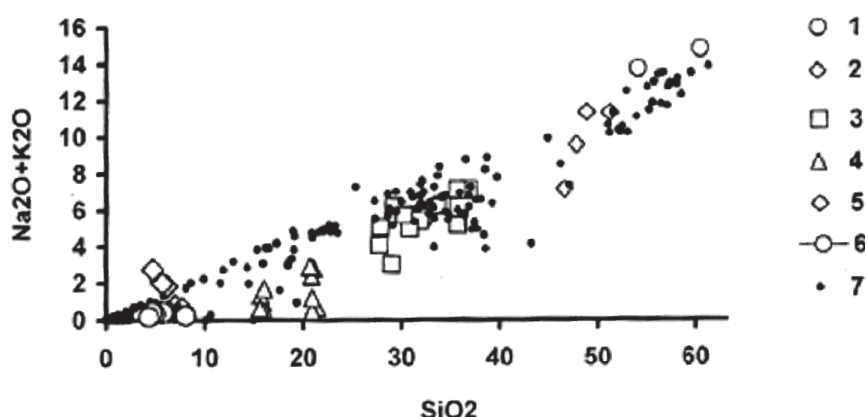


Fig. 15. Distribution of imaging points of control population ( $n = 200$ ) and cluster groups of main population of chemical analyses of the Tomtor field rocks:  
1–6 – the series of compositions of cluster groups; 7 – imaging points of control population.

It is critical to underscore, that analogous evolutionary curve in the  $\text{SiO}_2$ – $(\text{Na}_2\text{O}+\text{K}_2\text{O})$  coordinates is also typical of other polycarbonatite-containing complexes (Fig. 16).

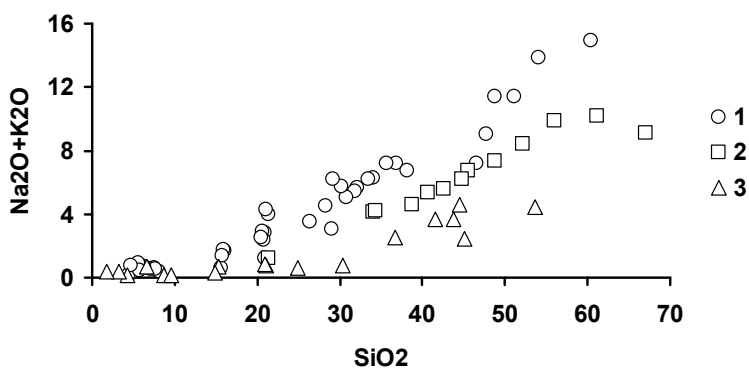


Fig. 16. Distribution of imaging points of averaged compositions of cluster groups:  
 1 – Tomtor; 2 – Oshurkovo apatite deposit; 3 – Seligdar apatite deposit.

The verification performed makes it possible to recommend the applied methodology of system approach for study and practical use (geological mapping) of other polycarbonate-containing complexes.

#### REFERENCES

1. Altschuller Z. S. Distribution of phosphorus in carbonatites / Z. S. Altschuller // Phosphorus in the Environment. – Moscow : Mir, 1977. – P. 47–56. (in Russian)
2. Apatite Rocks of Seligdar / V. B. Vasilenko, L. G. Kuznetsova, L. D. Kholodova [et al.]. – Novosibirsk : Nauka, 1982. – 215 p. (in Russian)
3. Baturin G. N. Phosphate Rocks on Bottom of Oceans / G. N. Baturin. – Moscow : Nauka, 1978. – 231 p. (in Russian)
4. Belousov A. F. Volcanic Formations / A. F. Belousov, A. P. Krivenko, Z. G. Polyakova. – Novosibirsk : Nauka, 1982. – 281 p. (in Russian)
5. Chetverikov S. D. Handbook on Petrochemical Recalculations of Rocks Analyses and Determination of Chemical Types of Rocks / S. D. Chetverikov. – Moscow : Gosnauchtekhizdat, 1956. – 245 p. (in Russian)
6. Classification of Kimberlites and Internal Structure of Kimberlite Pipes. – Moscow : Nauka, 1981. – 136 p. (in Russian)
7. Cramer H. Mathematical Methods of Statistics / H. Cramer. – Moscow : Mir, 1975. – 648 p. (in Russian)
8. Diday E. The dynamic clusters method in nonhierarchical clustering / E. Diday // Intern. J. Comp. Inform. Sci. – 1973. – N 2. – P. 61–88.
9. Epshtein E. M. Geology of unique Tomtor deposit of rare metals (North of the Siberian Platform) / E. M. Epshtein, N. A. Danilchenko, S. A. Postnikov // Geologiya Rudnyh Mestorozhdeniy (Rus.). – 1994. – Vol. 36, N 2. – P. 83–110.
10. Geological Vocabulary. Vol. 1. – Moscow : Nedra, 1978. – 486 p. (in Russian)
11. Kimberlites and Carbonatites. Collection of Studies on Petrochemistry / V. B. Vasilenko, L. G. Kuznetsova, V. A. Minin [et al.]. – Novosibirsk : Parallel, 2013. – 745 p. (in Russian)
12. Krumbein W. Models of Geological Processes / W. Krumbein, M. Kaufman, R. McCammon. – Moscow : Mir, 1973. – 149 p. (in Russian)

13. Kuznetsov Yu. A. Main Types of Magmatic Formations / Yu. A. Kuznetsov. – Moscow : Nedra, 1964. – 387 p. (in Russian)
14. McKelvey V. E. Occurrence and distribution of phosphorus in the lithosphere / V. E. McKelvey // Phosphorus in the Environment. – Moscow : Mir, 1977. – P. 24–46. (in Russian)
15. Method for estimating potential platinum content of stratified gabbroids based on petrochemical model / V. B. Vasilenko, A. P. Krivenko, L. G. Kuznetsova, L. D. Kholodova // Geologiya i Geofizika (Rus.). – 1995. – Vol. 36, N 12. – P. 73–79.
16. Perchuk L. L. Chemical relationship of fluids and magma / L. L. Perchuk // Fluids in Magmatic Processes. – Moscow : Nauka, 1982. – P. 269–280. (in Russian)
17. Petrochemistry of CaO and P<sub>2</sub>O<sub>5</sub> in kimberlites and genesis problem of Seligdar apatite rocks (Aldan) / V. B. Vasilenko [et al.] // Petrochemistry, Genesis and Ore-Bearing of Siberian Magmatic Formations. – Novosibirsk : Nauka, 1985. – P. 171–178. (in Russian)
18. Petrochemistry of Subalkaline Carbonatite-Bearing Complexes of Siberia / V. B. Vasilenko, N. N. Zinchuk, L. G. Kuznetsova, V. P. Serenko. – Novosibirsk : Nauka, 1994. – 231 p. (in Russian)
19. Razumova V. N. Ancient Weathering Crusts and Hydrothermal Process / V. N. Razumova. – Moscow : Nauka, 1977. – 156 p. (in Russian)
20. Standard quartz as a criterion of mass transfer intensity in postmagmatic change of Botuobinskaya pipe kimberlites / V. B. Vasilenko, A. V. Tolstov, V. A. Minin, L. G. Kuznetsova // Geologiya i Geofizika (Rus.). – 2008. – Vol. 49, N 12. – P. 1189–1204.
21. Tolstov A. V. Prospects for mining the Tomtor deposit of complex niobium-rare-earth ores / A. V. Tolstov, N. P. Pokhilenko // EKO (Rus.) – 2012. – N 11. – P. 17–27.
22. Zavaritsky A. N. Igneous Rocks / A. N. Zavaritsky. – Moscow : AN SSSR, 1955. – 479 p. (in Russian)

Стаття: надійшла до редакції 12.01.2016  
прийнята до друку 05.09.2016

## ПЕТРОХІМІЧНІ МОДЕЛІ КАРБОНАТИТІВ МАСИВУ ТОМТОР (СХІДНИЙ СИБІР)

**В. Василенко, Л. Кузнєцова, О. Толстов, В. Мінін**

*ФДБУН “Інститут геології і мінералогії ім. В. С. Соболєва СВ РАН”,  
просп. акад. Коптюга, 3, 630090 м. Новосибірськ, Росія  
E-mail: vasilenko@igm.nsc.ru*

Досліджено хімічний склад порід Томторського масиву (2 100 хімічних аналізів) за керном 193 свердловин, які розташовані вздовж лінії з південного сходу на північний захід масиву. Для виділення однорідних породних груп, якими складений масив, аналізи опрацьовано на підставі системного підходу із застосуванням методів математичної статистики. Попередньо базу даних хімічного складу порід розділено методом кластерного аналізу на 43 групи. Точки середнього складу груп у полі діаграми  $\text{SiO}_2-(\text{Na}_2\text{O}+\text{K}_2\text{O})$  розташовані в межах шести дискретних серій. Перша серія відповідає складу лужних сіенітів, друга – лужних габро, третя – мелілітоподібних порід, четверта–шоста серії представлені полігенними карбонатитами, які ми назвали полікарбонатитами. Усім серіям притаманні значні варіації складу, причому вони зростають у напрямі від третьої серії до першої та до шостої. Третю серію трактуємо як родонаочальну для всього масиву; вона сформувалася внаслідок селективного плавлення лужних базальтів за умов насичення  $\text{CO}_2$ . Ендогенна вугекислота була на всіх стадіях формування порід.

Окремо досліджено поведінку фосфору. Сформульовано петрохімічні критерії перевірки генетичних гіпотез утворення промислових скupчень фосфору. У досліджуваних породах виявлено гравітаційні (залишкові) та метасоматичні концентрації фосфору.

Доведено, що виділення серій порід виконано достовірно. Подібні петрохімічні серії наявні й на інших апатитових родовищах, тому їх можна використовувати, наприклад, під час геологічного картування.

**Ключові слова:** карбонатити, лужні породи, ультраосновні породи, системний підхід, математична статистика, генетичні гіпотези, родовища фосфору, Томторський масив, Східний Сибір.